

# Astro2020 Science White Paper

## Stellar Feedback in the ISM Revealed by Wide-Field Far-Infrared Spectral-Imaging

**Thematic Areas:**

Resolved Stellar Populations and their Environments

**Principal Author:**

Name: [Javier R. Goicoechea](#)

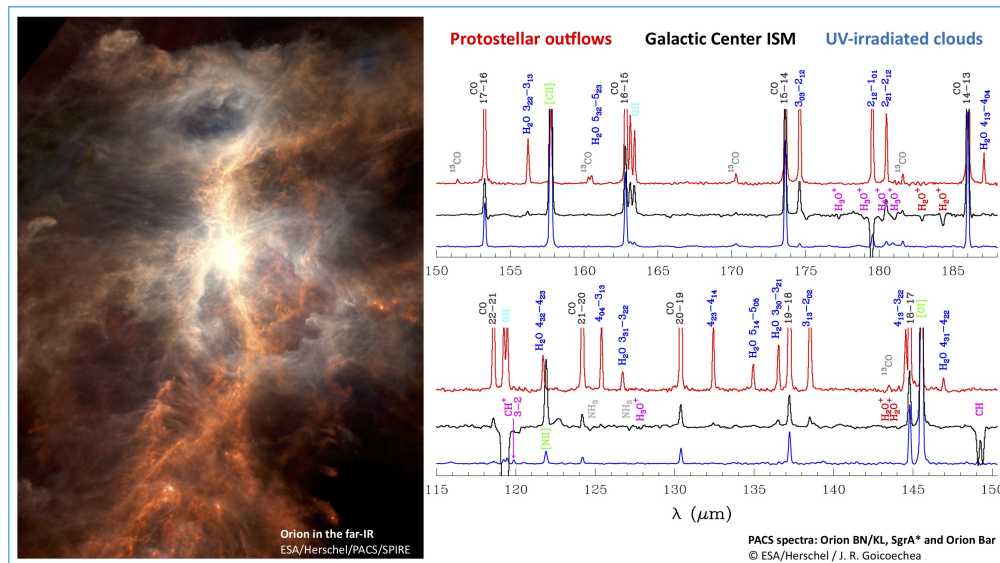
Institution: Instituto de Física Fundamental, CSIC, Madrid, Spain. Email: [javier.r.goicoechea@csic.es](mailto:javier.r.goicoechea@csic.es)

**Co-authors:**

[Maryvonne Gerin](#), Observatoire de Paris & CNRS, France.

[Emeric Bron](#), Observatoire de Paris-Meudon, France.

**Abstract:** The radiative and mechanical interaction of stars with their environment drives the evolution of the ISM and of galaxies as a whole. The far-IR emission ( $\lambda \simeq 30$  to  $350 \mu\text{m}$ ) from atoms and molecules dominates the cooling of the warm gas in the neutral ISM, the material that ultimately forms stars. Far-IR lines are thus the most sensitive probes of stellar *feedback* processes, and allow us to quantify the deposition and cycling of energy in the ISM. While *ALMA* (in the (sub)mm) and *JWST* (in the IR) provide astonishing sub-arcsecond resolution images of point sources and their immediate environment, they cannot access the main interstellar gas coolants, nor are they designed to image entire star-forming regions (SFRs). *Herschel* far-IR photometric images of the interstellar dust thermal emission revealed the ubiquitous large-scale filamentary structure of SFRs, their mass content, and the location of thousands of prestellar cores and protostars. These images, however, provide a *static* view of the ISM: not only they don't constrain the cloud dynamics, moreover they cannot reveal the chemical composition and energy transfer within the cloud, thus giving little insight into the regulation process of star formation by stellar feedback. In this *WP* we emphasize the need of a space telescope with wide-field spectral-imaging capabilities in the critical far-IR domain.



# 1. Far-IR Tracers of Stellar Feedback: Warm Molecular Gas

Massive stars dominate the injection of radiative and mechanical energy into the ISM through ionizing radiation, stellar winds, supernova explosions, and merger encounters (Beuther et al. 2007; Krumholz et al. 2014; Motte et al. 2018; Pabst et al. 2019; Zinnecker & Yorke 2007). This energy input shakes the environment, heats the gas, disrupts star-forming regions (SFRs), and creates the cloud and intercloud phases of the ISM. Massive stars are born inside giant molecular cloud (GMC) cores. Protostars of different masses develop inside these star-forming cores (e.g., McKee & Ostriker 2007). Their outflows shock the ambient cloud, heating and compressing the immediate environment around them. This is an example of small spatial scale protostellar feedback. Young stellar objects (YSOs) can be detected in photometric images by the bright far-IR/submm luminosity of their heavily obscured dusty cocoons.

On the large-spatial scales of an entire GMC, however, most of the gas and dust emission does not arise from individual YSOs but from the extended and more massive cloud component – the poorly known star-forming *environment*. Once a new massive star or cluster is formed, the energy and momentum injected by UV photoionization, radiation pressure, and stellar winds, ionize and erode the parental molecular cloud, creating H II regions and blowing expanding bubbles (see simulations in e.g., Krumholz et al. 2014; Rahner et al. 2017). Stellar feedback can thus determine the gas physical conditions and chemical composition at large scales, drive the evolution of the parental cloud itself, and regulate the formation of new stars. However, due to the lack of wide-field spectroscopic observations, there are fundamental aspects that remain to be understood. UV radiation in particular, is a very important player in the interaction of stars and ISM.

Photodissociation regions (PDRs) develop at the interfaces between the hot ionized gas and the cold molecular gas, and more generally, at any slab of neutral gas (hydrogen atoms not ionized) illuminated by stellar far-UV (FUV) photons with  $E < 13.6$  eV (Hollenbach & Tielens 1997). The famous far-IR [C II]158  $\mu\text{m}$  fine-structure line is typically the brightest emission from PDR gas, and it dominates the cooling of the neutral ISM at the scales of an entire galaxy. It thus provides key information on the energy deposited in the ISM (see *COBE*'s low resolution maps of the Milky Way, Bennett et al. 1994). With an ionization potential of 11.3 eV, however,  $\text{C}^+$  can also be abundant in both the warm neutral or ionized gas (e.g., Pineda et al. 2013). Hence, it is not always trivial to delimitate the origin of the [C II] 158  $\mu\text{m}$  emission and fully exploit its diagnostic power. Because of their specific chemistry, *certain molecular species that we discuss below, emitting in the far-IR, are very good filters of the different feedback processes.*

***Finding observational tracers of the feedback processes acting on the molecular gas, the fuel to form new stars, is crucial not only locally, but also in the framework of star formation across cosmic time.***

**Only in the far-IR and only from space.** While the low-energy molecular lines that can be detected from (sub)mm-wave ground-based radio telescopes such as ALMA typically trace cold and quiescent interstellar gas, the extended *warm molecular gas* ( $T_k \gtrsim 100$  K) affected by feedback processes (i.e., heated by stellar UV fields, enhanced X-ray doses, cosmic-ray particles, or affected by shocks and turbulence dissipation) naturally emits at higher frequencies, in the far-IR. The far-IR domain hosts a plethora of bright atomic fine-structure lines (from the neutral and ionized phases of the ISM) and high-energy (rotationally-excited) lines from CO,  $\text{H}_2\text{O}$ ,  $\text{CH}^+$ , HD, and other hydrides that cannot be detected from the ground. These far-IR lines, often the most luminous lines emitted by the ISM of galaxies as a whole, prove to be unique diagnostics of the different types of energy and momentum input deposited into the ISM. That is, of the different feedback mechanisms. The launch of ESA's *Infrared Space Observatory (ISO)* in 1995 opened the complete far-IR domain to spectroscopic observations, and demonstrated that the gas properties and energetics of YSOs can be constrained by studying their far-IR rotationally excited CO and  $\text{H}_2\text{O}$  line emission (e.g., Ceccarelli et al. 1996; Giannini et al. 2001). These lines are major coolants of the *hot* ( $T_k > 500$  K) molecular gas and the unambiguous signature of shocked gas (e.g., Kaufman & Neufeld 1996). IR  $\text{H}_2$  lines, observed by *ISO*, NASA's *Spitzer* and soon again with *JWST*, are also excellent tracers of the hot molecular

gas, but their emission is often heavily affected by dust extinction toward embedded protostars. *ISO* had a primary mirror of  $\sim 60$  cm size and carried primitive far-IR detectors. This limited the angular resolution and sensitivity of these pioneering detections. The launch of ESA’s *Herschel* in 2009, with a much larger  $\sim 3.5$  m telescope and equipped with more sophisticated far-IR instrumentation (direct detection detectors and heterodyne receivers) allowed a more robust characterization of (a rather short list of) low- and high-mass YSOs in different stages of evolution (e.g., van Dishoeck et al. 2011). However, robust statistics and spectroscopic observations of much larger protostellar samples and their environment are largely missing. More precisely, *Herschel* did not have instrumentation to carry out spectroscopic maps of entire star-forming regions.

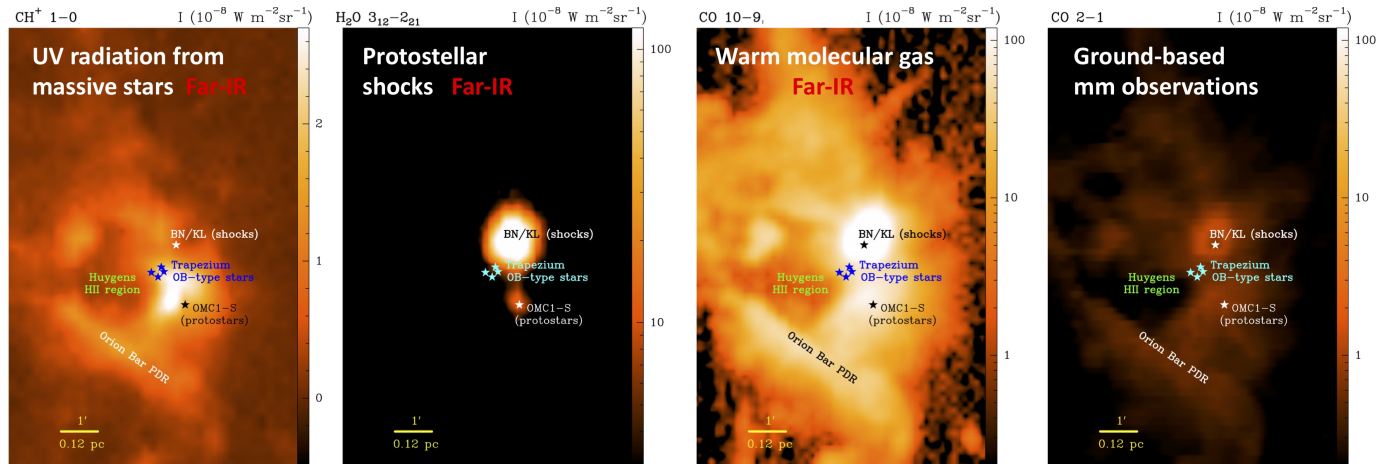


Figure 1: *Herschel* images of different molecular lines toward Orion (the closest high-mass star-forming region). They all show different spatial distributions:  $\text{CH}^+$  (UV-irradiated gas),  $\text{H}_2\text{O}$  (hot shocked gas),  $\text{CO } J = 10-9$  (extended warm gas) and  $\text{CO } J = 2-1$  (observed from the ground and much fainter).

Figure 1 shows  $\sim 85$  arcmin<sup>2</sup> images of key far-IR line obtained with the HIFI receiver toward the Orion molecular cloud core (OMC-1), the closest high-mass SFR (at  $\sim 414$  pc). These are one of the few spectroscopic-maps obtained by *Herschel* (Goicoechea et al. 2019). These images show the emission from  $\text{CH}^+$  (strongly FUV-irradiated gas),  $\text{H}_2\text{O}$  (hot shocked gas from protostellar outflows),  $\text{CO } J = 10-9$  (extended warm PDR gas) and  $\text{CO } J = 2-1$  (observed from the ground). The four emission lines show remarkably different spatial distributions, *emphasising the distinctive diagnostic power of different molecules and far-IR lines*. In the following, we briefly review the information that can be obtained *only* from far-IR line observations, and we apply it to our case: the radiative feedback from massive stars.

**$\text{H}_2\text{O}$  and OH** only reach high abundances in hot/warm shocked gas. Far-IR  $\text{H}_2\text{O}$  and OH rotational lines cover a broad range of energies and excitation conditions. Thus, they are excellent diagnostics of YSOs, and of shocks due to outflows in general: protostellar, supernovae or extragalactic (Sturm et al. 2011). Owing to the water vapor on Earth’s atmosphere, these lines can not be observed from the ground or with *SOFIA*.

**CO rotational ladder** can be used as a “thermometer” of the hot/ warm molecular gas. Far-IR high- $J$  CO lines have been detected by *ISO* and *Herschel* at different spatial scales: from outflows driven by nearby low-mass protostars to luminous active galactic nuclei (AGN) galaxies. In these energetic sources affected by shocks, the CO spectral line energy distribution (SLED) peaks at  $J > 15$  ( $\lambda < 173.6$   $\mu\text{m}$ ) and shows detectable emission at  $J > 30$  ( $\lambda < 87.2$   $\mu\text{m}$ , Hailey-Dunsheath et al. 2012; Karska et al. 2013). The CO line emission measured by *Herschel* toward less extreme SFRs, however, typically peaks at  $J \lesssim 10$  and shows large-scale emission as seen in nearby SFRs like Orion (see Fig. 1). When observed at high spectral resolution ( $< 1$  km s<sup>-1</sup>), mid- $J$  CO lines show narrow line-profiles, demonstrating that they arise from FUV-illuminated extended warm gas and not from fast shocks (e.g., Goicoechea et al. 2019).

**Hydrides such as  $\text{CH}^+$**  have their rotational lines in the far-IR. These molecules are not only important because their formation represents the first steps of interstellar chemistry (see Gerin et al. 2016). *Herschel* showed that their abundances are also unique tracers of the  $\text{H}_2$  column density (HF and CH), the ionization rate by cosmic-ray particles or X-rays ( $\text{OH}^+$ ,  $\text{H}_2\text{O}^+$  or  $\text{ArH}^+$ ), and the stellar FUV field ( $\text{CH}^+$  or  $\text{SH}^+$ ). In addition, the hydride emission from dense star-forming clouds ( $n_{\text{H}} > 1000 \text{ cm}^{-3}$ ) traces **gas components and physical conditions that cannot be studied from the ground**. One outstanding example is  $\text{CH}^+$ . The main gas-phase pathway producing detectable quantities of  $\text{CH}^+$  is reaction  $\text{C}^+ + \text{H}_2(v) \rightarrow \text{CH}^+ + \text{H}$ , where  $v$  refers to the specific  $\text{H}_2$  vibrational level (Agúndez et al. 2010; Sternberg & Dalgarno 1995). For  $\text{H}_2$  molecules in  $v=0$  state, this reaction is very endothermic,  $\Delta E/k \simeq 4300 \text{ K}$ , much higher than the typical gas temperatures of molecular clouds. However, the reaction becomes exothermic and fast for  $v \geq 1$ . Observations and theory show that UV photons from nearby massive stars can radiatively pump  $\text{H}_2$  to vibrationally excited states  $v \geq 1$  over large spatial-scales. In consequence,  $\text{CH}^+$  can be abundant at large scales too, and its emission can be used to characterize the stellar UV radiation field (Goicoechea et al. 2019). In particular,  $\text{CH}^+$  probes a narrow (low  $A_V$ ) but very extended component of UV-irradiated molecular cloud surfaces (where not all carbon is locked in CO).  $\text{CH}^+$  is clearly a unique tracer of harsh interstellar conditions. Not surprisingly,  $\text{CH}^+$  ( $J=1-0$ ) emission has been detected by ALMA toward high-redshift ULIRG galaxies (Falgarone et al. 2017). Hence,  $\text{CH}^+$  can also be used to constrain the energetics of the primitive ISM.

**Radiative Feedback and PDRs:** Most of the mass contained in GMCs resides at low visual extinction depths ( $A_V$ ). Therefore, most of the gas is permeated by stellar FUV photons. A strong FUV radiation field from nearby massive stars induces a plethora of poorly understood dynamical effects and chemical changes in the cloud. The high thermal pressures inferred from *Herschel* observations toward a few H II/PDR interfaces,  $P_{\text{th}} = T_k \cdot n_{\text{H}} \gtrsim 10^7 - 10^9 \text{ cm}^{-3} \text{ K}$ , are consistent with the expected dynamical response of molecular clouds to strong FUV radiation: the cloud edges are heated and compressed, and photoevaporate if the high pressures are not balanced by those of the environment (Bertoldi & Draine 1996; Bron et al. 2019). Cloud photoevaporation models predict that the thermal pressure at the irradiated cloud edges scales with the strength of the FUV flux impinging the cloud (see Fig. 2).  $\text{CH}^+$ , a very reactive and short-lived molecule, proves to be as a unique tracer of these narrow layers, clearly revealing feedback processes. In particular, Goicoechea et al. (2019) found a spatial correlation between the intensity of the  $\text{CH}^+$  emission and  $G_0$ , the flux of FUV photons (Fig. 2). The observed correlation is supported by PDR models in the parameter space  $P_{\text{th}}/G_0 \approx [5 \cdot 10^3 - 8 \cdot 10^4] \text{ cm}^{-3} \text{ K}$  where many observed PDRs lie (Joblin et al. 2018).

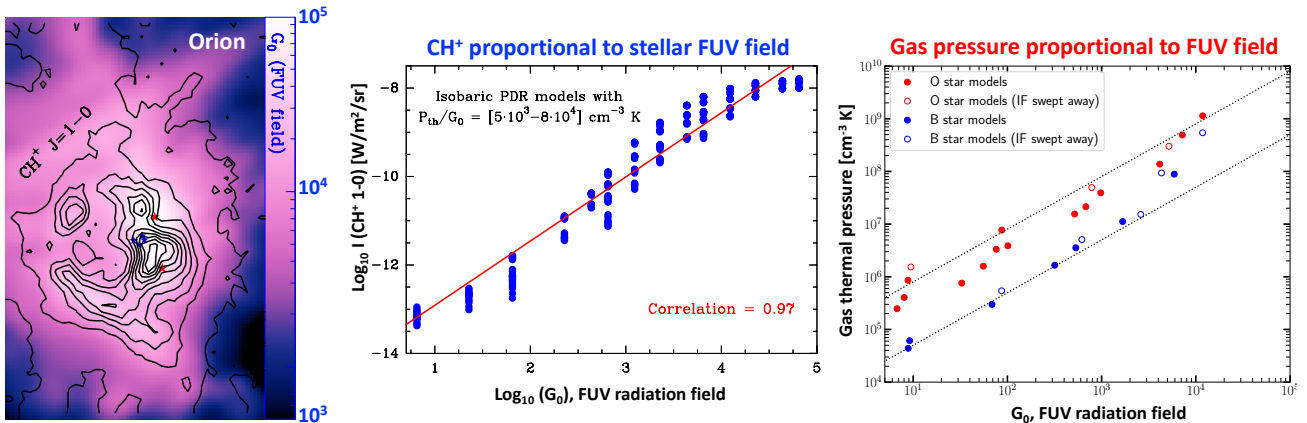


Figure 2: *Left:* FUV radiation field ( $G_0$ ) arising from OB-type stars in Orion’s Trapezium cluster. Black contours are the  $\text{CH}^+$  ( $J = 1-0$ ) emission observed by *Herschel* and showing a very good spatial correlation with  $G_0$ . *Middle:* This correlation is supported by PDR models (Goicoechea et al. 2019). *Right:*  $P_{\text{th}}$  vs.  $G_0$  correlation at the edge of FUV-illuminated clouds predicted by photoevaporation models (Bron et al. 2019).

## 2. Need and feasibility of far-IR spectral-imaging capabilities

The ISM is a central component of galaxies; it provides the fuel to form new stars and it keeps a relic of previous star generations in the form of metal enrichment. Dust extinction hides the star and planet formation processes from UV, visible-light, and often near-IR observations. Stellar UV radiation, winds and supernova explosions heat and disrupt the interstellar environment, sometimes enhancing, sometimes quenching the star formation processes. The main gas coolants in these environments emit in the far-IR (e.g., Schneider et al. 2018). The peak of the dust emission also lies in the far-IR ( $\lambda \simeq 100 \mu\text{m}$  for  $T_d \simeq 30 \text{ K}$ ). Therefore, *the far-IR is the natural domain to study the ISM lifecycle and stellar feedback. Since these processes take place at large-spatial scales, spectral-imaging capabilities are desperately needed. Single-dish space telescopes are the obvious choice for mapping and accessing the complete wavelength domain at high sensitivity and stability.* The spectacular large-scale photometric-images of the dust emission taken by *Herschel*'s far-IR cameras provided a static “snapshot” of the star-formation processes. However, these images say less about the stellar feedback processes in the ISM, and how to quantify them. It is only by carrying out large spatial scale far-IR observations of the critical gas cooling lines, and of other key astrochemical probes such as  $\text{CH}^+$ , that we will be able to quantify these processes and their energetics. In addition, by using sub-km s<sup>-1</sup> velocity-resolution spectrometers similar to *Herschel*/HIFI or *SOFIA*/GREAT receivers, we will also be able to constrain the gas kinematics and turbulence properties (see e.g., Goicoechea et al. 2019; Pabst et al. 2019).

**The future.** Neither *ISO* nor *Herschel* could carry out wide-field spectral-imaging observations. The new generation multi-beam instruments on board *SOFIA* or balloon experiments, combined with efficient on-the-fly (OTF) mapping techniques, will allow faster and larger maps. However, these stratospheric telescopes do not cover the entire far-IR domain (e.g., they can't observe  $\text{H}_2\text{O}$  or  $\text{CH}^+$ ), they are severely limited by the available flying time (e.g., they can't map the Galactic plane in reasonable times), and they are restricted to the detection of a few bright lines. To overcome these issues, several far-IR space-telescope concepts have been conceived to probe the ISM lifecycle and stellar feedback, some adapted to the bright and extended emission of the Milky Way and nearby galaxies, others pushing beyond to characterize the ISM of distant and primitive galaxies (see e.g., the EU far-IR Space Roadmap, Rigopoulou et al. 2017):

- (1.) A  $\sim 1$  m-class space telescope equipped with multi-beam heterodyne receivers (thus providing sub-km s<sup>-1</sup> spectral resolution) and employing OTF techniques to scan very large areas of the Milky Way's galactic plane and provide velocity-resolved images of the interstellar gas in the brightest gas cooling lines simultaneously (see e.g., Rigopoulou et al. 2016, for the *FIRSPEX* concept).
- (2.) A cooled  $\sim 2.5$  m-class space telescope equipped with a very sensitive grating spectrometer, accessing the entire far-IR band at medium spectral resolution, but providing very little spectral multiplexing capabilities (see e.g., Roelfsema et al. 2018, for the *SPICA* concept).
- (3.) A cooled  $\sim 6$  m-class space telescope equipped with ultra-sensitive grating spectrometers accessing the entire far-IR band for wide-field spectral-imaging at low-spectral resolution ( $R$  of a few hundred) or at higher  $R$  for single beam observations (see e.g., Battersby et al. 2018, for the *OST* concept).

Concept (1.) is specifically designed for mapping the galactic ISM, and is only limited by sensitivity and available bandwidth to simultaneously map  $N$  lines. Concept (3.), if equipped with multi-beam heterodyne receivers, will fulfil the science cases presented in this WP. Concept (2.) or (3. without receivers) will be able to detect all relevant far-IR gas cooling lines, retrieving their line intensities (thus accessing the gas energetics) but not the gas kinematics or line-profile information. Even at low to medium  $R$ , they will detect the far-IR atomic and molecular lines from the warm interstellar gas and from hundreds of protostars, and propoplanetary disks. This has been demonstrated by previous observations toward Orion with the grating spectrometers *ISO*/LWS ( $R \simeq 200$ ) and *Herschel*/PACS ( $R \simeq 2000$ ). Future instruments of this kind, however, will have to develop spectral-imaging techniques as efficient as possible (e.g., using steering mirrors).

**Science case:** With the exception of a few far-IR spectral-maps toward nearby and bright high-mass SFRs, almost all square-degree areas of the Milky Way covered by *Herschel* far-IR dust photometric images do not have spectroscopic counterpart in the main gas cooling lines ([C II] 158  $\mu\text{m}$ , [O I] 63  $\mu\text{m}$ ) and in critical molecular line tracers of stellar feedback (high- $J$  CO lines, H<sub>2</sub>O, CH<sup>+</sup>...). In order to fill this gap, we propose a program to carry out spectral-imaging of the most relevant high-mass SFRs of the Galaxy (typically located a kpc distances) and also to map young superclusters in nearby galaxies (e.g., 30 Dor in the LMC). As an example, here we focus on the CO  $J=12-11$  ( $E_u/k = 431$  K) line at  $\lambda=217$   $\mu\text{m}$ . This is the first CO rotational line that could be detected by a instrument such as *SPICA*/*SAFARI*, but we note that the highest-energy lines at  $J > 50$  would be detectable too. In addition to the many CO and H<sub>2</sub>O lines available in the far-IR band, other key target lines are CH<sup>+</sup>  $J=1-0$ , 2-1, 3-2 and 4-3 (at  $\lambda=359$ , 179.6, 119.8, and 90.0  $\mu\text{m}$  respectively) and HD  $J=1-0$  and 2-1 (at  $\lambda=112.0$  and 56.2  $\mu\text{m}$  respectively).

In this example, we require to map a  $\sim 75$  pc<sup>2</sup> area of several template GMCs. This would imply scanning angular sizes of  $50' \times 50'$  for massive SFRs like W51 (at a distance of 5 kpc), but sizes of  $5' \times 5'$  toward GMCs of the LMC. *Herschel* observations show that the *extended* warm molecular gas emission in Orion (at only 0.5 kpc) produces surface brightness of  $\sim 10^{-8}$  W m<sup>-2</sup> sr<sup>-1</sup> in the mid- $J$  CO lines (see Fig. 1). Assuming extended emission filling the beam of the different types of telescope concepts ( $\sim 1$ ,  $\sim 2.5$ , and  $\sim 6$  m telescope sizes), we compute the line flux sensitivity needed to detect this emission level toward SFRs of increasing distance (of course some regions will have a brighter or a fainter line emission level depending on the particular excitation conditions and dominant feedback processes). Expectations are shown in Figure 3. Just for reference, we note that the line sensitivity of *Herschel*/PACS was several times  $10^{-18}$  W m<sup>-2</sup> ( $5\sigma/1$  hr). We see that in order to detect the warm molecular gas emission beyond the Galactic Center with a  $\sim 2.5$  m telescope, we require line sensitivities of several  $10^{-19}$  W m<sup>-2</sup>, and an order of magnitude better to image the molecular ISM of nearby galaxies. While the smaller telescope concept will be more flexible to map degree-size areas of the Milky Way at parsec-scale spatial resolution, a  $\sim 6$  m telescope improves by a factor of  $\sim 2$  the angular resolution provided by *SOFIA* or *SPICA*. This will allow us reaching, for the first time in far-IR spectral line maps, a  $\sim 0.1$  pc ( $\sim 20,000$  AU) spatial resolution for all SFRs at distances below 2.5 kpc. This scale has been suggested to be the universal width of the filaments that build up the structure of star-forming clouds (e.g., Arzoumanian et al. 2011). In addition, such kind of telescope will allow us to spatially resolve the emission from hundreds of protostars and their outflows.

High-mass star-forming region	<i>Carina</i>	<i>W51</i>	<i>W49N</i> and <i>Galactic Center</i>	<i>30 Dor</i> (LMC)	
Distance to source	$\sim 2.5$ kpc	$\sim 5$ kpc	$\sim 10$ kpc	$\sim 50$ kpc	
Size of a $\sim 75$ pc cloud map	100' x 100'	50' x 50'	25' x 25'	5' x 5'	Angular resolution @ CO $J=12-11$
Spatial resolution Line Flux (W m <sup>-2</sup> beam <sup>-1</sup> ) (1m telescope, <i>FIRSPEX</i> )	0.5 pc 2.7E-17	1.0 pc 6.7E-18	1.9 pc 1.7E-18	9.6 pc 6.7E-20	54"
Spatial resolution Line Flux (W m <sup>-2</sup> beam <sup>-1</sup> ) (2.5m telescope, <i>SPICA</i> )	0.2 pc 4.3E-18	0.4 pc 1.1E-18	0.8 pc 2.7E-19	3.8 pc 1.1E-20	22"
Spatial resolution Line Flux (W m <sup>-2</sup> beam <sup>-1</sup> ) (6m telescope, <i>OSt</i> )	0.1 pc 7.4E-19	0.2 pc 1.9E-19	0.3 pc 4.7E-20	1.6 pc 1.9E-21	9"

**Stellar feedback in SFRs and ISM**

How are molecular clouds disrupted and how does this relate to the presence of nearby massive stars?

How does feedback affect star formation?

What is the pressure in ISM clouds and how is it regulated?

What are the relative roles of radiative and mechanical heating?

What are the properties of the H<sup>+</sup>/H/H<sub>2</sub> interfaces in the ISM?

Figure 3: Wide-field far-IR spectral-imaging of template high-mass star-forming regions. We propose to map a  $\sim 75$  pc<sup>2</sup>-size SFR with three far-IR space telescope concepts. The resolution and required line sensitivity are based on the CO  $J=12-11$  line at  $\lambda \simeq 217$   $\mu\text{m}$  and its observed intensity toward Orion.

## References

- Agúndez, M., Goicoechea, J. R., Cernicharo, J., Faure, A., & Roueff, E. 2010, *ApJ*, 713, 662
- Arzoumanian, D., André, P., Didelon, P., et al. 2011, *A&A*, 529, L6
- Battersby, C., Armus, L., Bergin, E., et al. 2018, *Nature Astronomy*, 2, 596
- Bennett, C. L., Fixsen, D. J., Hinshaw, G., et al. 1994, *ApJ*, 434, 587
- Bertoldi, F. & Draine, B. T. 1996, *ApJ*, 458, 222
- Beuther, H., Churchwell, E. B., McKee, C. F., & Tan, J. C. 2007, *Protostars and Planets V*, 165
- Bron, E., Agúndez, M., Goicoechea, J. R., & Cernicharo, J. 2019, submitted to *A&A*, astro-ph/1801.01547
- Ceccarelli, C., Hollenbach, D. J., & Tielens, A. G. G. M. 1996, *ApJ*, 471, 400
- Falgarone, E., Zwaan, M. A., Godard, B., et al. 2017, *Nature*, 548, 430
- Gerin, M., Neufeld, D. A., & Goicoechea, J. R. 2016, *AR&A*, 54, 181
- Giannini, T., Nisini, B., & Lorenzetti, D. 2001, *ApJ*, 555, 40
- Goicoechea, J. R., Santa-Maria, M. G., Bron, E., et al. 2019, *A&A*, 622, A91
- Hailey-Dunsheath, S., Sturm, E., Fischer, J., et al. 2012, *ApJ*, 755, 57
- Hollenbach, D. J. & Tielens, A. G. G. M. 1997, *ARA&A*, 35, 179
- Joblin, C., Bron, E., Pinto, C., et al. 2018, *A&A*, 615, A129
- Karska, A., Herczeg, G. J., van Dishoeck, E. F., et al. 2013, *A&A*, 552, A141
- Kaufman, M. J. & Neufeld, D. A. 1996, *ApJ*, 456, 611
- Krumholz, M. R., Bate, M. R., Arce, H. G., et al. 2014, *Protostars and Planets VI*, 243
- McKee, C. F. & Ostriker, E. C. 2007, *ARA&A*, 45, 565
- Motte, F., Bontemps, S., & Louvet, F. 2018, *ARA&A*, 56, 41
- Pabst, C., Higgins, R., Goicoechea, J. R., et al. 2019, *Nature*, 565, 618
- Pineda, J. L., Langer, W. D., Velusamy, T., & Goldsmith, P. F. 2013, *ApJ*, 554, A103
- Rahner, D., Pellegrini, E. W., Glover, S. C. O., & Klessen, R. S. 2017, *MNRAS*, 470, 4453
- Rigopoulou, D., Caldwell, M., Ellison, B., et al. 2016, in *SPIE*, Vol. 9904, *Space Telescopes and Instrumentation 2016: Optical, Infrared, and Millimeter Wave*, 99042K
- Rigopoulou, D., Helmich, F., Hunt, L., et al. 2017, *arXiv e-prints*, 1701.00366
- Roelfsema, P. R., Shibai, H., Armus, L., et al. 2018, *PASA*, 35, e030
- Schneider, N., Röllig, M., Simon, R., et al. 2018, *A&A*, 617, A45
- Sternberg, A. & Dalgarno, A. 1995, *ApJS*, 99, 565
- Sturm, E., González-Alfonso, E., Veilleux, S., et al. 2011, *ApJL*, 733, L16
- van Dishoeck, E. F., Kristensen, L. E., Benz, A. O., et al. 2011, *PASP*, 123, 138
- Zinnecker, H. & Yorke, H. W. 2007, *ARA&A*, 45, 481